Low noise high-T_c superconducting bolometers on silicon nitride membranes for far-infrared detection

M. J. M. E. de Nivelle,[a] M. P. Bruijn, R. de Vries, J. J. Wijnbergen, and P. A. J. de Korte
Space Research Organization Netherlands, Sorbonnelaan 2, 3584 CA Utrecht, The Netherlands

S. Sánchez and M. Elwenspoek
MESA Research Institute, Twente University, P.O. Box 217, 7500 AE Enschede, The Netherlands

T. Heidenblut and B. Schwierzi
Institut für Halbleitertechnologie und Werkstoffe der Elektrotechnik, Universität Hannover, Appelstrasse 11A, D-30167 Hannover, Germany

W. Michalke and E. Steinbeiss
Institut für Physikalische Hochtechnologie, Helmholtzweg 4, D-07743 Jena, Germany

(Received 27 June 1997; accepted for publication 6 August 1997)

High-T_c $GdBa_2Cu_3O_{7-\delta}$ superconductor bolometers with operation temperatures near 89 K, large receiving areas of 0.95 mm^2 and very high detectivity have been made. The bolometers are supported by 0.62 μm thick silicon nitride membranes. A specially developed silicon-on-nitride layer was used to enable the epitaxial growth of the high-T_c superconductor. Using a gold black absorption layer an absorption efficiency for wavelengths between 70 and 200 μm of about 83% has been established. The noise of the best devices is fully dominated by the intrinsic phonon noise of the thermal conductance G, and not by the $1/f$ noise of the superconducting film. The temperature dependence of the noise and the resulting optimum bias temperature have been investigated. In the analysis the often neglected effect of electrothermal feedback has been taken into account. The minimum electrical noise equivalent power (NEP) of a bolometer with a time constant τ of 95 ms is 2.9 $pW/Hz^{1/2}$ which corresponds with an electrical detectivity D^* of 3.4×10^{10} cm $Hz^{1/2}/W$. Similar bolometers with $\tau=27$ ms and NEP=3.8 $pW/Hz^{1/2}$ were also made. No degradation of the bolometers could be observed after vibration tests, thermal cycling and half a year storage. Measurements of the noise of a Pr doped $YBa_2Cu_3O_{7-\delta}$ film with $T_c=40$ K show that with such films the performance of air bridge type high-T_c bolometers could be improved. © *1997 American Institute of Physics.* [S0021-8979(97)03322-7]

I. INTRODUCTION

For the detection of far-infrared radiation both thermal detectors and nonthermal photovoltaic (photon) detectors can be used.[1] Usually photon detectors are preferred but their spectral response is limited by the cutoff wavelength $\lambda_c = hc/U_c$, with U_c the charge carrier excitation energy. This implies that for long wavelength response U_c must be very small. At the same time the operating temperature must be low enough so that the thermal energy kT is much smaller than the excitation energy. Typically, for operation at liquid nitrogen temperature (77 K) HgCdTe detectors are used with a cutoff wavelength of about 12 μm and a detectivity D^* at 10 μm of 2×10^{10} cm $Hz^{1/2}/W$. For longer wavelengths up to 200 μm doped Si or Ge photon detectors are used with operating temperatures below 10 K.

At higher operating temperatures and longer wavelengths photon detectors are outperformed by thermal detectors. Above 77 K probably the highest detectivity over the broadest band in the far-infrared can be achieved with high-T_c superconducting transition edge bolometers. In these bolometers the temperature is read out with a high-T_c superconductor, making use of the very high temperature coefficient of resistance at the superconducting transition.

During the last years a lot of effort has been put into the development and optimization of these detectors.[1–6] The highest detectivity $D^*=A^{1/2}/\mathrm{NEP}=8\times10^9$ cm $Hz^{1/2}/W$ is reported for a detector with a sensitive area A of 50×50 μm^2 and a NEP (noise equivalent power) for radiation with wavelengths between about 12 and 36 μm of 6.3×10^{-13} $W/Hz^{1/2}$ at a frequency of 32 Hz.[5]

Possible applications of high-T_c bolometers which can be cooled with liquid nitrogen or small low power mechanical cryocoolers, exist in far-infrared spectroscopy in laboratory or in space-based systems.

We have investigated bolometers which consist of a 0.6–1 μm silicon nitride (silicon rich Si_xN_y) membrane with a high-T_c superconducting $GdBa_2Cu_3O_{7-\delta}$ (GBCO) film on top. The operating temperature (near the midpoint of the superconducting transition) is about 89 K. Si_xN_y has been chosen because very strong membranes can be made of it and because its thermal conductivity is very low, making a high sensitivity possible. A 300 nm monocrystalline silicon layer on top of the Si_xN_y membrane enables the epitaxial growth of the superconductor. This is necessary for a low level of the $1/f$ noise of the high-T_c film. A gold black absorption layer is deposited on the detector to obtain a high efficiency in the far-infrared.[7]

The bolometers described here are intended for a possible satellite instrument for remote sensing of atmospheric

[a]Electronic mail: m.denivelle@sron.ruu.nl

OH.[8,9] It is one of the instruments investigated in the PI-RAMHYD study (Passive Infra-Red Atmospheric Measurements of HYDroxyl) of the European Space Agency. PI-RAMHYD aims at global monitoring of important species in the atmospheric chemistry by limb sounding of the emitted radiation. In the instrument a Fabry-Perot etalon together with a reflection grating is used to select the 84.42 μm emission line of OH.

II. BOLOMETER THEORY

Recently, excellent reviews of the theory have been published.[1,2] However, in these and most other publications the effect of electrothermal feedback on the noise properties as noted by Mather[10] is neglected. Especially for transition edge bolometers the influence of this feedback can be substantial.[11,12] So, a brief presentation of the theory is given in which the influence of feedback on the noise has been taken into account in a more accessible manner than by Mather.

A bolometer is a thermal detector, which employs an electrical resistance thermometer to measure the temperature of a radiation absorber. Depending on the ratio between its characteristic time constant τ and the time τ_g between the arrival of the individual energy carriers (photons or particles) it will operate like a calorimeter or a bolometer.[2] Here we will focus on the second case, where $\tau/\tau_g \gg 1$.

The bolometer consists of an absorbing volume with heat capacity C [J/K] which is weakly coupled to a cold bath at temperature T_0 by a link with thermal conductance G [W/K]. The resulting thermal time constant τ [s] is equal to C/G. The bolometer contains a resistive thermometer which is characterized by its temperature coefficient of resistance α given by

$$\alpha = \frac{1}{R}\frac{dR}{dT}\,[\mathrm{K}^{-1}]. \tag{1}$$

The thermometer is readout by measuring the current through or the voltage over the thermometer. In the first case the bolometer is ideally biased with a constant voltage, in the second case with a constant current.

The functional behavior is described and clarified by the block diagram in Fig. 1. In this diagram $\Delta P = \eta \Delta P_{\mathrm{rad}}$ is the absorbed radiation (η is the absorption efficiency). The separate (Laplace) transfer functions for the transfer from power to temperature (F_1), from temperature variation to variation of the thermometer resistance (F_2), from resistance variation to the output voltage or current (F_3) and from output voltage or current to electrical power dissipated in the thermometer (F_4) are indicated. The Fourier equivalent for F_1 describing the thermal relaxation is $(1/G)/(1+i\omega\tau)$. The feedback loop takes account of the electrical dissipation in the thermometer which adds up to the input signal. The text between the brackets holds for the case of current bias with voltage readout, and the alternatives without brackets for voltage bias with current readout.

In case of current bias with voltage readout the open loop gain $A = F_1 F_2 F_3$ is given by

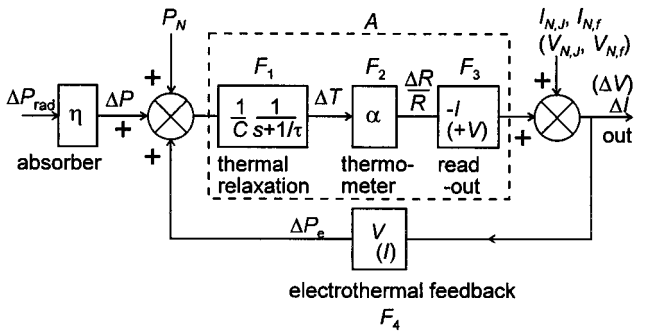

FIG. 1. Functional block diagram of a bolometer. The text between the brackets holds for current bias with voltage readout, the alternatives without brackets for voltage bias with current readout. The contributions to the signal from phonon noise (P_N) of the thermal conductance G, and from Johnson and $1/f$ noise ($V_{N,J}$ and $V_{N,f}$, respectively, $I_{N,J}$ and $I_{N,f}$) of the thermometer resistance are also indicated.

$$A = \frac{V\alpha}{G}\frac{1}{1+i\omega\tau}\,[\mathrm{V/W}], \tag{2}$$

and the loop gain $L = AF_4$ is

$$L = \frac{P\alpha}{G}\frac{1}{1+i\omega\tau} = L_0\frac{1}{1+i\omega\tau}, \tag{3}$$

with $L_0 = P\alpha/G$. $P = IV$ is the bias power. Instead of L_0 the symbol a is often used. The responsivity S of the bolometer is equal to the closed loop gain which is given by

$$S = \frac{A}{1-L} = \frac{1}{I}\frac{L_0}{1-L_0}\frac{1}{1+i\omega\tau_e}\,[\mathrm{V/W}], \tag{4}$$

where $\tau_e = \tau/(1-L_0)$ is the effective thermal time constant. It follows that for stable operation L_0 must be smaller than 1. This implies that for a positive temperature coefficient α (which is the case for a superconducting thermometer biased at its transition temperature T_c) there is a maximum to the bias current. In literature $L_0 = 0.3$ is often regarded as close to the optimum.

In case of voltage bias with current readout the responsivity becomes

$$S = -\frac{1}{V}\frac{L_0}{1+L_0}\frac{1}{1+i\omega\tau_e}\,[\mathrm{A/W}], \tag{5}$$

with $\tau_e = \tau/(1+L_0)$ and $L_0 = V^2\alpha/RG$. Now L_0 must be larger than -1. This means that in case of a positive temperature coefficient α there is no limit for the bias voltage. By increasing the bias power P the speed of the bolometer can be increased with a factor $1+L_0$.[11] If L_0 is large the bolometer is operated in so-called extreme electrothermal feedback mode.[12]

The sensitivity of a bolometer is limited by various noise sources: Johnson noise and $1/f$ noise of the thermometer resistance, phonon noise of the thermal conductance G, fluctuations of the background radiation, and external noise from the measurement system including amplifiers, load resistance, fluctuations in the bath temperature, etc.[1,2] For high-T_c bolometers the most important noise contributions are the

phonon, the $1/f$ and the Johnson noise. Their input in the bolometer feedback loop is shown in the block diagram of Fig. 1.

The phonon noise power P_N is given by

$$P_N = \mathrm{NEP}_p = (\gamma 4kT^2G)^{1/2} \ [\mathrm{W/Hz^{1/2}}], \tag{6}$$

where $\gamma = 1$ for small temperature gradients over the thermal conductance G.[10] The resulting voltage noise at the output equals

$$V_{N,p} = |S|(\gamma 4kT^2G)^{1/2} \ [\mathrm{V/Hz^{1/2}}]. \tag{7}$$

In case of current bias the Johnson noise of the thermometer resistance generates a noise voltage

$$V_{N,J} = (4kTR)^{1/2} \ [\mathrm{V/Hz^{1/2}}]. \tag{8}$$

Due to the electrothermal feedback this noise term is modified at the output by a factor $1/(1-L)$ which is usually neglected in literature:

$$V^*_{N,J} = \frac{V_{N,J}}{1-L} = V_{N,J}(1+IS). \tag{9}$$

Here the second term can be recognized as the response of the bolometer to the power which is dissipated by the constant bias current in the Johnson noise source. The resulting NEP due to the Johnson noise referred to the input of the loop is

$$\mathrm{NEP}_J = \frac{V^*_{N,J}}{|S|} = \frac{V_{N,J}}{|A|} = (4kTP)^{1/2}\frac{1}{|L_0|}|1+i\omega\tau| \ [\mathrm{W/Hz^{1/2}}]. \tag{10}$$

It can be shown that exactly the same result holds for voltage bias with current readout. Note that the time constant which plays a role is τ rather than τ_e.

A similar discussion holds for the $1/f$ (excess) noise of the thermometer. By substituting for $V_{N,J}$ the $1/f$ voltage noise

$$V_{N,f} = \sqrt{\frac{c}{f}}\,V \tag{11}$$

it is found that the NEP due to the $1/f$ noise equals

$$\mathrm{NEP}_f = \sqrt{\frac{c}{f}}\frac{G}{\alpha}|1+i\omega\tau|. \tag{12}$$

A useful empirical relation for the parameter c is[13]

$$c = \frac{\gamma_H}{n_c E}, \tag{13}$$

with γ_H the Hooge parameter, n_c the charge carrier concentration, and E the volume of the resistor. The minimum of NEP_f is found at a frequency $f = 1/2\pi\tau$.

In order to reach the sensitivity limit set by the phonon noise, NEP_J should be smaller than NEP_p. From Eqs. (6) and (10) it follows that this condition is fulfilled (at $f = 1/2\pi\tau$) if

$$T > \frac{2}{\alpha L_0}. \tag{14}$$

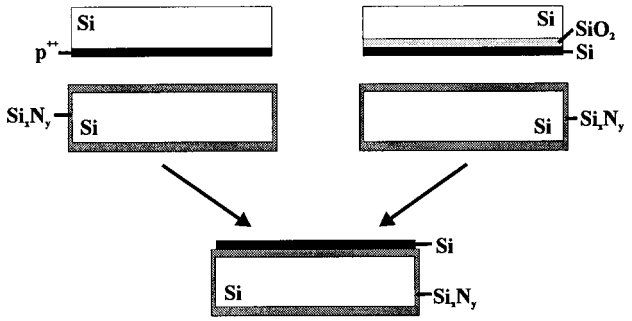

FIG. 2. Two routes for silicon-on-nitride production, using a $p++$ layer (left) or a SOI wafer (right).

For the investigated high-T_c bolometers this is practically always true since for current bias L_0 is typically 0.3, and α about $2\,\mathrm{K^{-1}}$ around the midpoint of the superconducting transition ($T \sim 90$ K).

Analogously, by requiring that the phonon noise exceeds the $1/f$ noise at $f = 1/2\pi\tau$ it is found that [Eqs. (6), (12), and (13)]

$$\frac{\gamma_H}{n_c E} < \frac{kT^2\alpha^2}{\pi C}. \tag{15}$$

This condition can be fulfilled in a temperature window around the superconducting transition where the bolometer has the lowest NEP, as will be discussed in Sec. V C.

III. PRODUCTION PROCESS

High-T_c $GdBa_2Cu_3O_{7-\delta}$ transition edge bolometers on micromachined Si membranes have been reported, with an operating temperature of about 85 K.[4] These bolometers have a receiving area of 0.85×0.85 mm^2, a NEP of 3×10^{-11} W/Hz$^{1/2}$ and a time constant of 0.4 ms. The quality parameter[6] $D^*/\tau^{1/2} = 1.4\times10^{11}$ cm/s W is the highest value found in literature for high-T_c bolometers. Their large sensing area as compared to most other high-T_c bolometers[3,5,6] with typical sizes between 50×50 and 100×100 μm^2 makes them very suitable for detection of radiation with relatively long wavelengths of 100 μm and above.

Based on this design we have developed a new bolometer with an equally large receiving area but with a much lower NEP. This has been achieved by replacing the supporting silicon by silicon nitride which has a much lower thermal conductivity. A problem imposed by this change is the fact that a thin single crystalline Si layer is needed on top of the amorphous silicon nitride, to allow epitaxial growth of the superconductor. To obtain this layer a new bond-and-etch-back technique[14] involving a fusion bonding step between a silicon nitride layer (Si_xN_y) and Si has been developed.[15–17]

The 0.62 μm low-stress Si_xN_y layer is grown by low pressure chemical vapor deposition. Prior to the bonding the surface roughness of the Si_xN_y is reduced by chemical mechanical polishing. As shown in Fig. 2 two different methods are used to obtain the thin Si layer after bonding-and-etch-back: boron implantation yielding a stop layer for etching in a solution of KOH with iso-propyl alcohol (route 1), and

using the buried oxide layer of a commercially obtained silicon-on-insulator (SOI) wafer as an etch stop in a KOH solution (route 2). More details of these processes are published elsewhere.[17]

To obtain a high quality superconductor, a 40 nm epitaxial yttria stabilized ZrO_2 (YSZ) buffer layer with a top layer of CeO_2 was first grown on the Si. Subsequently, the YSZ/CeO_2 and Si layers are patterned by argon ion milling and reactive ion etching, respectively, thereby defining the layout of the GBCO thermometer. On the buffer a 60 nm GBCO is deposited by magnetron sputtering. Only on the parts where the Si/YSZ/CeO_2 layer is still present, this film is superconducting, whereas outside this region on the amorphous silicon nitride it is insulating (inhibit technique).

Subsequently the structure is covered *in situ* by a 200 nm PtO_x passivation layer. On the bond pads the PtO_x is reduced to metallic Pt by local laser heating. At this point the superconducting transition temperature and the transition width of the samples are tested, resulting in a yield of good quality samples of about 70%.

Next the membrane is etched in KOH, with the sample mounted in a front side protection chuck. The yield of this etching process is over 70%. Most of the failures had a clear cause, which could be avoided in the following runs.

The final production step is the deposition of an absorption layer on the membrane. Without this layer the expected absorption efficiency is only around 13%–26%.[4] We use a gold black layer made by evaporation of gold in a nitrogen environment of 8 mbar.[7] The porous gold black layer has a filling fraction of about 0.3%. A shadow mask is used to define a circular absorption area with a diameter of 1.1 mm. In Fig. 3 a top view of the detector area of a produced bolometer is shown.

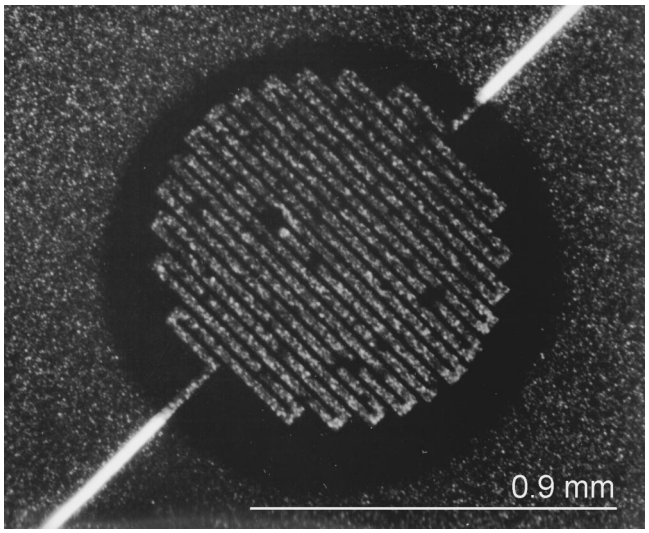

FIG. 3. Optical micrograph of the central part of a $3\times3\,\mathrm{mm}^2$ bolometer membrane with a 25 μm wide GBCO meander. The meander is just visible through the porous 35 μm thick gold black absorption layer, which covers an area with a diameter of 1.1 mm.

IV. MEASUREMENTS

A. Measurement setup

The bolometers are characterized in a vacuum cryostat with liquid nitrogen cooling. The bolometer temperature can be controlled with 1 mK resolution. On a time scale of 100 s temperature fluctuations are less than 5 μK. Connections to the platinum contact pads of the bolometer are made with bonded gold wires. For low frequency noise measurements the bolometers are connected in a bridge setup, using a 1 kHz ac bias current and lock-in amplification. With this setup the system noise spectrum is flat down to at least 0.1 Hz.

The optical response of the bolometer is calibrated with the difference signal from two filtered black bodies at about 30 and 50 °C. The total radiation power from these black bodies which is collected on the bolometer is about 1.0 and 1.1 μW, respectively. For filtering we use a cold filter consisting of 1 mm quartz and a set of polyethylene scatter filters with diamond, KCl, NaF, and LiF powder. The resulting spectrum covers a band from about 70 to 200 μm, with a maximum at 85 μm and a cut-off edge at 65 μm. The radiation with wavelengths below 65 μm adds less than 2% to the total calibration signal. To concentrate the radiation on the absorber a Winston cone is used, with the exit opening of 1.1 mm diameter positioned in front of the absorber at a distance less than 0.2 mm.

B. Results

Eight bolometers have been characterized, two of them with $3\times3\,\mathrm{mm}^2$ membranes, the others with $2\times2\,\mathrm{mm}^2$ membranes. Three bolometers have a noise level which is fully dominated by the phonon noise, with the $1/f$ noise $V_{N,f}$ of the superconducting film less than 30% of the phonon noise voltage $V_{N,p}$. For the other bolometers ratios between 0.8 and 1.8 were determined. These sample-to-sample variations

TABLE I. Summary of results for five bolometers. The membranes of bolometers 4 and 5 are $3\times3\,\mathrm{mm}^2$, the others are $2\times2\,\mathrm{mm}^2$. Noise values and responsivity are given for $f=1/2\pi\tau$. The column f_{range} gives the frequency range over which NEP is minimal. NEP_o is the optical NEP, equal to NEP/η.

No.	G [μW/K]	τ [ms]	T [K]	R [kΩ]	α [K^{-1}]	L_0	S [kV/W]	V_N [nV/Hz$^{1/2}$]	NEP [pW/Hz$^{1/2}$]	f_{range} [Hz]	$V_{N,f}/V_{N,p}$	black [μm]	η [%]	NEP_o [pW/Hz$^{1/2}$]
1	33	27	85.7	3.9	1.0	0.47	6.5	25	3.8	1.5-13	0.2	0	…	…
2	45	22	87.5	2.0	3.5	0.38	6.5	30	4.6	0.6–13	0.3	0	18	24
3	42	37	88.2	0.49	3.2	0.31	2.8	17	6.0	0.8–9	1.0	24	62	9.7
4	18	95	89.9	1.9	5.8	0.19	8.4	25	2.9	0.2–3	0.3	0	26	11
5	15	115	89.9	3.6	3.8	0.09	6.9	26	3.8	0.2–2	0.9	35	69	5.5

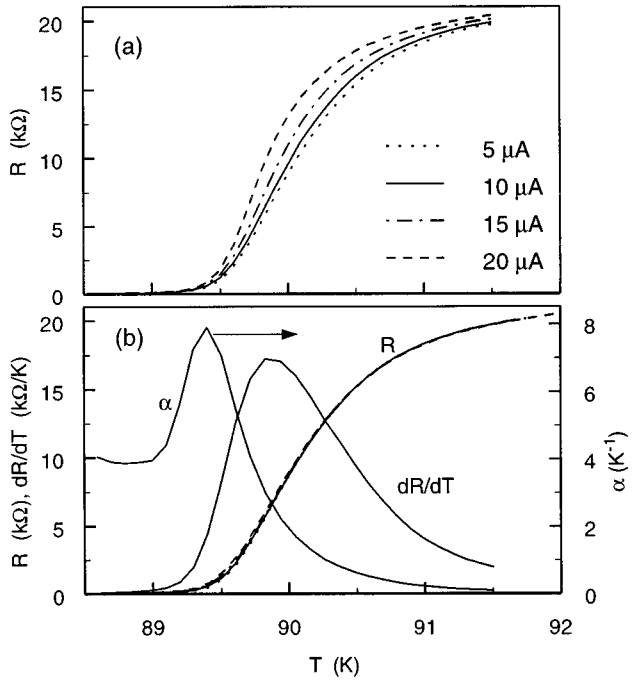

FIG. 4. Resistance of a bolometer, for different bias currents as a function of temperature T, where (a) T is the bath (substrate) temperature T_0; (b) T is the membrane temperature given by $T=T_0+I^2R/G$, with $G=1.8\times10^{-5}$ W/K.

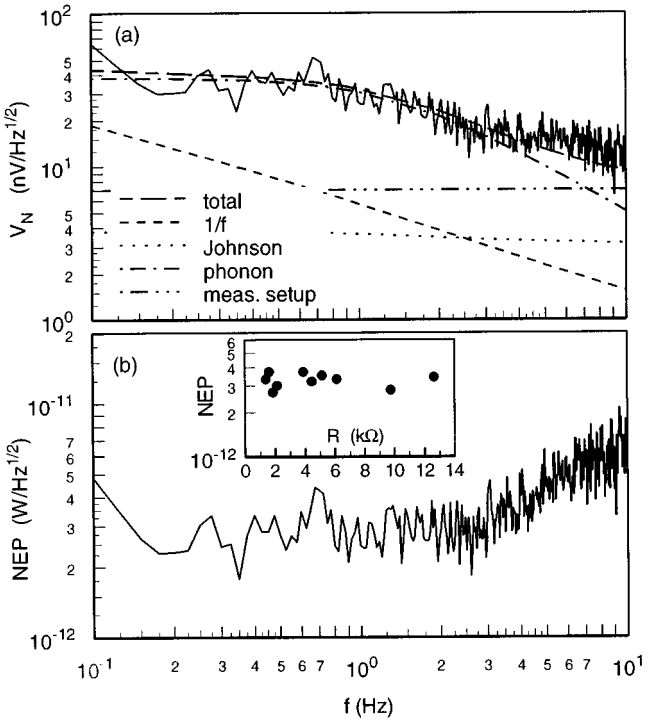

FIG. 5. (a) Noise spectrum at $T_0=89.5$ K, $I=17.8$ mA, $R=1.89$ kΩ. Furthermore $dR/dT=11.0$ kΩ/K, $L_0=0.19$, and $|S|=8.4$ kV/W at $\omega=1/\tau$ [Eq. (4)]. Also shown are the calculated spectra of the phonon noise and Johnson noise, a fitted $1/f$ noise spectrum and the noise of measurement setup, and their orthogonal sum. (b) Corresponding frequency spectrum of the (electrical) NEP. The bump around 0.7 Hz is generated by the measurement setup. The inset shows the NEP at $\omega=1/\tau$ for different bias points in the $R(T)$ transition.

must be related to for instance grain boundaries and inhomogeneities in the high-T_c film. The results of five bolometers are summarized in Table I. We will focus on the performance of the bolometers with the lowest $1/f$ noise level.

The resistance versus temperature for different bias currents of a bolometer (No. 4, Table I) with a 3×3 mm^2 membrane and a GBCO meander with a length of 17 mm and a width of 25 μm is shown in Fig. 4. In Fig. 4(a) the temperature T_0 of the substrate is plotted. In Fig. 4(b) the temperature has been corrected for the temperature rise of the membrane due to resistive heating: $T=T_0+I^2R/G$, where G is the fitted value of the thermal conductance for which the $R-T$ curves coincide. In this way a value of G equal to 1.8×10^{-5} W/K has been determined. The time constant $\tau=C/G$ is 95 ms. This value is calculated from the measured effective rise time $\tau_e=\tau/(1-L_0)$ of the bolometer response to an on-off switching LED.

By subtracting the thermal conductivity of the 0.32 μm Si layer underneath the contact leads (with $\kappa\approx10$ W/cm K[18]) a thermal conductivity for the Si_xN_y of about 0.030 W/cm K is estimated. At the temperature where dR/dT is maximal, the temperature coefficient of resistance α is 2.5 K^{-1} and the resistivity ρ is 50 $\mu\Omega$ cm. The critical current density of the superconductor measured before membrane etching is about 1.3×10^6 A/cm^2 at 77 K. These are typical values for good quality $YBa_2Cu_3O_{7-\delta}$ (YBCO) or GBCO films.

Voltage noise spectra $V_N(f)$ of the detector have been measured for different bias currents and different temperatures in the superconducting transition region. A typical spectrum is shown in Fig. 5(a). Also, the spectra of the phonon noise and Johnson noise which are calculated with Eqs. (7) and (9) are shown. It can be seen that between about 0.2 and 3 Hz the measured spectrum is fully dominated by the phonon noise.

The corresponding electrical NEP$(f)=V_N(f)/|S(f)|$ is plotted in Fig. 5(b). Between 0.2 and 3 Hz the NEP is about 2.9 pW/Hz$^{1/2}$, which is almost equal to NEP$_p$ [Eq. (6)]. In the inset it is shown that the NEP is approximately constant over a broad range of bias points in the superconducting transition. A further discussion of the temperature dependence follows in Sec. V C.

The bolometer efficiencies for wavelengths between 70 and 200 μm of some bolometers with different gold black absorption layers have been measured. In Fig. 6 the effective efficiency η is plotted versus the thickness of the absorption layer. η is calculated as the ratio of the measured dc responsivity $\Delta V/\Delta P_{\rm rad}$ and the calculated responsivity $|S|$ at $\omega=0$ [Eq. (4)].

For G, in the calculations of $|S|$, the thermal conductivities between meander and heat sink (i.e., the rim of the membrane) have been used as obtained with fits to $R(T)$ data taken at different electrical power levels [see Figs. 4(a) and 4(b)]. These values are not influenced by the deposition of the gold black layers. However, the optical power is absorbed over a larger area (with diameter $d_a=1.1$ mm) than the electrical power ($d_m=0.9$ mm), so that the effective

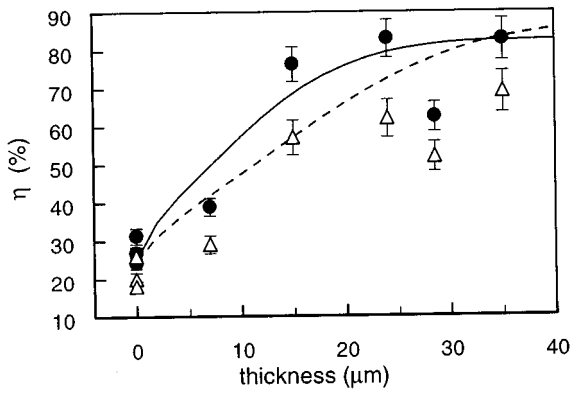

FIG. 6. Observed bolometer efficiencies η (triangles) vs the thickness of the gold black absorption layer. The solid circles are the corresponding real absorption efficiencies $\tilde{\eta}$ obtained by correcting for the larger G between absorber and substrate than between meander and substrate. The curves are the calculated absorption efficiencies of the complete bolometer sandwich. Solid line: calculated for a conductivity σ of the gold black of 300 $\Omega^{-1}\mathrm{m}^{-1}$; dashed line: $\sigma = 100\ \Omega^{-1}\mathrm{m}^{-1}$.

thermal conductivity for the optical measurements is different from the electrical one. So, the effective optical efficiency η has to be corrected by a factor $\ln(D/d_m)/\ln(D/d_a)$, with D the outer diameter of a circular membrane with the same area as the square bolometer membrane, in order to get the optical efficiency $\tilde{\eta}$ of the gold black. The resulting absorption efficiencies $\tilde{\eta}$ are plotted in the same figure.[19]

It is seen that above a gold black thickness of about 25 μm the efficiency saturates near 83%. This is in good agreement with the reflectivity of 10%–20% at 85 μm wavelength obtained with separate measurements of the diffuse reflectivity of gold black layers deposited on reflecting metal substrates.

Also shown are the calculated absorption efficiencies for two values of the electrical conductivity of the gold black. These two values ($\sigma = 100$ and $\sigma = 300\ \Omega^{-1}\mathrm{m}^{-1}$) are the extreme values of the measured conductivities of separate test samples. A reasonable agreement is seen between the determined absorption efficiencies and the calculated curve for $\sigma = 300\ \Omega^{-1}\ \mathrm{m}^{-1}$.

In the calculations the bolometer is modeled as a multilayer consisting of $\mathrm{Si}_x\mathrm{N}_y$ (thickness 620 nm) with a complex index of refraction $\tilde{n} = 2$,[20] covered for 45% with Si (320 nm, $\tilde{n} = 3.5$) and GBCO (60 nm, $\tilde{n} = 20 + i30$), and for 55% with high Ohmic GBCO (60 nm, estimation: $\tilde{n} = 3$). These fractions take account of the patterning of the silicon and the superconductor (neglecting diffraction near the edges). The refractive index of the superconducting GBCO is found as a fit parameter for the absorption without gold black. The GBCO layers are covered by PtO_x [200 nm, $\tilde{n} = 3.5 + i1.5$ (Ref. 21)] and gold black. The refractive index of the gold black layer was calculated with the effective dielectric function given by Becker with substitution of the measured electrical conductivity of the gold black.[7] Only specular reflection is considered. To take account of the Winston cone optics we have integrated over all angles of incidence between 0 and $\pi/2$, with a $2 \sin\phi \cos\phi$ weight function.

From the time constants of the bolometers before and after deposition of the gold black it could be determined that the specific heat of the black is only 6 mJ/cm^3 K. This corresponds with a filling fraction of 0.3%. The total heat capacity of a 1.1 mm diameter absorber with 25 μm thickness is only 1.4×10^{-7} J/K.

V. DISCUSSION

A. Influence of SON layer type

SON substrates made according to both routes in Fig. 2 have been used for the production of the bolometers. Measurements on both bolometer types do not indicate a clear difference in quality of the high-T_c film. This means that the crystal defects caused by the boron implantation do not influence the epitaxial growth of the high-T_c film. The only difference between the two bolometer types can be found in the heat conductance. The route 1 SON layer contains a highly boron doped silicon layer, which has a lower thermal conductivity than the low doped Si top layer of the SOI wafer.

B. Stress relief

The transition temperatures of both bolometers on a 3×3 mm^2 membrane are about 1.5 K higher than the typical transition temperatures of bolometers on 2×2 mm^2 membranes. It was also observed that the critical temperatures before membrane etching, with the GBCO thermometer still positioned on a solid substrate, and after, when it is positioned on a thin membrane, are different: after etching the T_c is about 1 K higher. Both observations suggest that as a result of the membrane etching there is some relaxation of the tensile stress in the meander which is caused by the differences in thermal expansion between the GBCO film and the Si substrate. Consequently T_c increases. The increase is surprisingly large: values around 0.4 K/GPa are reported for the pressure dependence dT_c/dP of $\mathrm{YBa_2Cu_3O_{7-\delta}}$ films (at ambient pressure and $0 < \delta < 0.1$),[22] while the calculated tensile stress in an YBCO film on a silicon substrate is only 0.9 GPa.[23]

C. Temperature dependence of noise

From fits to the measured noise spectra [Fig. 5(a)] we have determined the Hooge parameter γ_H of several samples. In Fig. 7 the Hooge parameters $\gamma_H(T)$ of two bolometers ($E = 2.5 \times 10^{-8}$ cm^3) are plotted versus $\alpha(T)$. For reference the data of a typical GBCO meander on a solid Si substrate are shown ($E = 3.5 \times 10^{-8}$ cm^3). An arbitrary value of 2×10^{21} cm^{-3} was used for the charge carrier density n_c in Eq. (13).

The determined Hooge parameters γ_H of the GBCO films are consistent with the values found in literature of high quality films.[9] The measured increase of γ_H with α can be compared with for instance the relation $\gamma_H \propto \alpha^2$ predicted by the thermal fluctuation model of Voss and Clarke.[24]

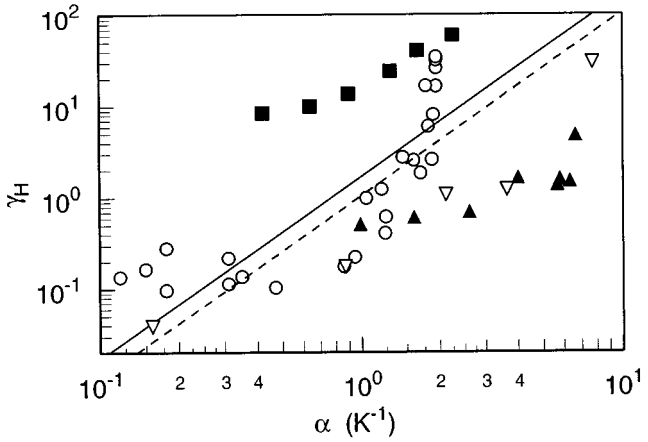

FIG. 7. Determined Hooge parameters $\gamma_H(T)$ vs $\alpha(T)$ of different samples (Table I). Circles: bolometer 1; solid triangles: bolometer 4; open triangles: GBCO film on solid substrate; solid squares: Pr doped YBCO film with $T_c = 40$ K; lines: calculated points where phonon noise and $1/f$ noise are equal for bolometer 1 (solid) and bolometer 4 (dashed).

For both bolometers the lines are shown which correspond to the ratio γ_H/α^2 where phonon and $1/f$ noise are equal [Eq. (15), with $T \approx T_c$]. It follows that in both cases there is a rather wide range in α or a temperature range in the superconducting transition where the $1/f$ noise is smaller than the phonon noise.

Also, the data are shown of a $Y_{0.6}Pr_{0.4}Ba_2Cu_3O_{7-\delta}$ meander with $T_c = 40$ K which we prepared on a Si substrate ($E = 3.5 \times 10^{-8}$ cm^3). This film is investigated because at 40 K, which is still in the range of Stirling cycle cryocoolers, the detector will be faster due to a reduced C (the thermal conductivity of the involved materials stays approximately constant), and the phonon noise will be reduced proportionally with T.

As far as we know there are no reports in literature on the Hooge parameters of doped YBCO films with reduced T_c. Given the sharp transition of the doped film, with $\alpha = 1.3$ K^{-1} and $\rho = 30$ $\mu\Omega$ cm at the temperature where dR/dT is maximum, we assume that the Hooge parameters here determined are typical for epitaxial and homogeneous $Y_{0.6}Pr_{0.4}Ba_2Cu_3O_{7-\delta}$ films. The optimum ratio γ_H/α^2 equals 14 K^2. Substitution in Eq. (15) yields $E/C > 1.0$ cm^3 K/J. For the investigated bolometer design a reduction of the heat capacity by a factor 3 is expected when cooling down from 90 to 40 K. This gives $E/C \approx 0.08$ cm^{3}K/J which is too small, so that the bolometer will be dominated by the $1/f$ noise. Only in detectors with a lower heat capacity, for instance with an air bridge design,[6] it might be possible to come close to the phonon noise limit. This would enable an increase of the speed with a factor 3 and a decrease of the NEP with a factor 2 by replacing the YBCO film with a doped film with $T_c \approx 40$ K.

D. Reduction of heat conductance

The measured NEP is dominated by the phonon noise, which scales with $G^{1/2}$ [Eq. (6)]. In the investigated design the two most important sources for this heat conductance are the silicon leads ($G \approx 9 \times 10^{-6}$ W/K) present underneath the contact leads from the meander structure to the bond pads, and the supporting silicon nitride membrane (also $G \approx 9 \times 10^{-6}$ W/K). The contribution from the silicon depends on both the size of the beams and the electrical conductivity of the silicon used.

By using higher doped Si and making the leads thinner and less wide a reduction of G_{Si} down to about 6×10^{-7} W/K seems feasible. The contribution from the silicon nitride can be reduced by patterning the membrane, thus obtaining a smaller membrane, suspended by narrow beams. Therefore experiments are started to produce free-standing suspension structures. Structures with 16 silicon nitride legs of 10 μm width and 1.5 mm length have already been made. The expected G_{SiN} is about 3.2×10^{-7} W/K so that the total G is about 1×10^{-6} W/K and the NEP around 0.7 pW/Hz$^{1/2}$.

The cost for the reduced NEP is a large time constant of about 2 s. By making use of voltage bias with large electrothermal feedback this time constant can potentially be reduced by a factor $1 + L_0$ [Eq. (5)] while keeping the NEP the same.[11] Using a bath temperature of 50 K we estimate a possible reduction from 2 s to about 50 ms. To reach the required low noise level with current readout probably a (high-T_c) SQUID current amplifier is necessary.

E. Stability

Several experiments have been done to test the stability of the bolometers. Some bolometers have been repeatedly cycled between room temperature and 80 K. After cycling no change in properties was seen. Also a bolometer which was remeasured after 6 months of storage showed no change in performance. Vibrating a gold black absorber at 30 g_{rms} for 2 minutes (white spectrum between 100 and 300 Hz, with main resonance peak at 2050 Hz) had no effect on the reflectivity ($\approx 14\%$). Vibrating a bolometer at 10 g_{rms} for 2 minutes had no effect on its $R(T,I)$ and noise properties.

VI. CONCLUSION

We have shown that high-T_c bolometers can be made on silicon nitride membranes with an output noise level which is dominated by the fundamental phonon noise. For frequencies between 0.2 and 3 Hz the achieved electrical NEP of 2.9 pW/Hz$^{1/2}$ is equal to the theoretical minimum determined by the phonon noise of the thermal conductance $G = 1.8 \times 10^{-5}$ W/K between the high-T_c thermometer and heat sink.

We have shown that an optical efficiency in the far-infrared around 83% can be obtained by depositing a gold black absorption layer on top of the bolometer membrane. The minimal required thickness of the gold black is about 25 μm. The filling fraction of the layer is 0.3%.

The lowest measured optical NEP ($\tau = 115$ ms) is 5.5 pW/Hz$^{1/2}$ which corresponds with a detectivity D^* of 1.8×10^{10} cm Hz$^{1/2}$/W. In this particular bolometer $1/f$ and phonon noise are approximately equal. With a gold black absorption layer deposited on a 3×3 mm^2 bolometer with negligible $1/f$ noise an optical NEP of 4.1 pW/Hz$^{1/2}$ and D^* of 2.4×10^{10} cm Hz$^{1/2}$/W are expected. The time constant is approximately 100 ms. For a bolometer with a 2×2 mm^2

membrane we calculate an optical NEP of 6.1 pW/Hz$^{1/2}$ and D^* of 1.6×10^{10} cm Hz$^{1/2}$/W, with $\tau\approx32$ ms.

The developed detector covers a very broad wavelength range of at least 70 to 200 μm. For this wavelength range and operating temperature they outclass other detectors like HgCdTe or stressed Ge:Ga detectors.

ACKNOWLEDGMENTS

This work was supported with funding of the Earth Observation Preparatory Program of the European Space Agency. The contract manager is Dr. E. Armandillo. We would like to thank W. Becker for helping us with his expertise on gold black deposition, and C. Gui for the chemical mechanical polishing investigations.

[1] P. L. Richards, J. Appl. Phys. **76**, 1 (1994).
[2] H. Kraus, Semicond. Sci. Technol. **9**, 827 (1996).
[3] B. R. Johnson, M. C. Foote, H. A. Marsh, and B. D. Hunt, Proc. SPIE **2267**, 24 (1994).
[4] H. Neff, J. Laukemper, I. A. Khrebtov, A. D. Tkachenko, E. Steinbeiss, W. Michalke, M. Burnus, T. Heidenblut, G. Hefle, and B. Schwierzi, Appl. Phys. Lett. **66**, 2421 (1995).
[5] S. J. Berkowitz, A. S. Hirahara, K. Char, and E. N. Grossmann, Appl. Phys. Lett. **69**, 2125 (1996).
[6] L. Méchin, J. C. Villégier, and D. Bloyet, J. Appl. Phys. **81**, 7039 (1997).
[7] W. Becker, R. Fettig, A. Gaymann, and W. Ruppel, Phys. Status Solidi B **194**, 241 (1996).
[8] J. J. Wijnbergen, P. A. J. de Korte, and M. J. M. E. de Nivelle, Proc. SPIE **2478**, 306 (1995).
[9] P. A. J. de Korte, M. J. M. E. de Nivelle, and J. J. Wijnbergen, Proc. SPIE **2578**, 294 (1995).
[10] J. C. Mather, Appl. Opt. **21**, 1125 (1982).
[11] A. T. Lee, P. L. Richards, S. W. Nam, B. Cabrera, and K. D. Irwin, Appl. Phys. Lett. **69**, 1801 (1996).
[12] K. D. Irwin, Appl. Phys. Lett. **66**, 1998 (1995).
[13] F. N. Hooge, T. G. M. Kleinpenning, and L. K. J. Vandamme, Rep. Prog. Phys. **44**, 479 (1981).
[14] C. A. Bang, J. P. Rice, M. I. Flik, D. A. Rudman, and M. A. Schmidt, J. Microelectromech. Syst. **2**, 160 (1993).
[15] M. J. M. E. de Nivelle, M. P. Bruijn, M. Frericks, R. de Vries, J. J. Wijnbergen, P. A. J. de Korte, S. Sánchez, M. Elwenspoek, T. Heidenblut, B. Schwierzi, W. Michalke, and E. Steinbeiss, J. Phys. IV **6**, 423 (1996).
[16] S. Sánchez, C. Gui, and M. Elwenspoek, J. Micromech. Microeng. **7**, 111 (1997).
[17] S. Sánchez, M. Elwenspoek, C. Gui, M. J. M. E. de Nivelle, R. de Vries, P. A. J. de Korte, M. P. Bruijn, J. J. Wijnbergen, W. Michalke, E. Steinbeiss, T. Heidenblut, and B. Schwierzi, J. Microelectromech. Syst. (in press).
[18] Y. S. Touloukian, *Thermophysical Properties of Matter: Thermal Conductivity, Nonmetallic Solids* (IFI/Plenum, New York, 1970).
[19] The deviation of the datapoint at 28.5 μm is probably due to an experimental error (e.g., optical misalignment): the datapoint belongs to the same bolometer as the datapoint at 35 μm which was obtained after deposition of an additional gold black layer on top of the first layer.
[20] Estimated value, various sources.
[21] H. Neff, S. Henkel, E. Hartmannsgruber, E. Steinbeiss, W. Michalke, K. Steenbeck, and H. G. Schmidt, J. Appl. Phys. **79**, 7672 (1996).
[22] C. C. Almasan, S. H. Han, B. W. Lee, L. M. Paulius, M. B. Maple, B. W. Veal, J. W. Downey, A. P. Paulikas, Z. Fisk, and J. E. Schirber, Phys. Rev. Lett. **69**, 680 (1992).
[23] W. Prusseit, S. Corsépius, M. Zwerger, P. Berberich, H. Kinder, O. Eibl, C. Jaekel, U. Breuer, and H. Kurz, Physica C **201**, 249 (1992).
[24] R. F. Voss and J. Clarke, Phys. Rev. B **13**, 556 (1976).